The EMBO Journal Vol.16 No.1 pp.83–97, 1997

Functional characterization of the Cdc42p binding domain of yeast Ste20p protein kinase

Ekkehard Leberer[1], Cunle Wu, Thomas Leeuw, Anne Fourest-Lieuvin, Jeffrey E.Segall[2] and David Y.Thomas

Eukaryotic Genetics Group, Biotechnology Research Institute, National Research Council of Canada, 6100 Royalmount Avenue, Montreal, Quebec H4P 2R2, Canada and [2]Department of Anatomy and Structural Biology, Albert Einstein College of Medicine, 1300 Morris Park Avenue, Bronx, NY 10461, USA

[1]Corresponding author

Ste20p from *Saccharomyces cerevisiae* belongs to the Ste20p/p65^{PAK} family of protein kinases which are highly conserved from yeast to man and regulate conserved mitogen-activated protein kinase pathways. Ste20p fulfills multiple roles in pheromone signaling, morphological switching and vegetative growth and binds Cdc42p, a Rho-like small GTP binding protein required for polarized morphogenesis. We have analyzed the functional consequences of mutations that prevent binding of Cdc42p to Ste20p. The complete amino-terminal, non-catalytic half of Ste20p, including the conserved Cdc42p binding domain, was dispensable for heterotrimeric G-protein-mediated pheromone signaling. However, the Cdc42p binding domain was necessary for filamentous growth in response to nitrogen starvation and for an essential function that Ste20p shares with its isoform Cla4p during vegetative growth. Moreover, the Cdc42p binding domain was required for cell–cell adhesion during conjugation. Subcellular localization of wild-type and mutant Ste20p fused to green fluorescent protein showed that the Cdc42p binding domain is needed to direct localization of Ste20p to regions of polarized growth. These results suggest that Ste20p is regulated in different developmental pathways by different mechanisms which involve heterotrimeric and small GTP binding proteins.

Keywords: Cdc42p/mating pheromone/signal transduction/Ste20p kinase/yeast

Introduction

The mating response of the haploid yeast *Saccharomyces cerevisiae* provides a genetically tractable model system to study a G-protein regulated mitogen-activated protein (MAP) kinase cascade. This response is initiated by the pheromones **a** and α-factor released from *MAT***a** and *MAT*α cells, respectively. These short polypeptides bind to cell type-specific receptors and thereby trigger the activation of a heterotrimeric G-protein that is common to both cell types (for a review, see Herskowitz, 1995). The β and γ subunits of the G-protein then activate a MAP kinase cascade consisting of Ste7p (a MAP kinase kinase or MEK homolog), Ste11p (a MEK kinase homolog) and the partially redundant MAP kinase homologs Fus3p and Kss1p (Herskowitz, 1995). The Ste20p protein kinase (a MEK kinase kinase) (Leberer *et al.*, 1992a; Wu *et al.*, 1995), Ste5p (Leberer *et al.*, 1993; Whiteway *et al.*, 1995) and Ste50p (Ramezani Rad *et al.*, 1992) play crucial roles in the activation of this MAP kinase cascade which ultimately regulates the Ste12p transcription factor (Dolan *et al.*, 1989) and Far1p, a negative regulator of cyclin/Cdc28 (Chang and Herskowitz, 1990).

This signaling pathway induces differentiation processes required to initiate conjugation of cells with opposite mating types. These cellular processes, which are typical of differentiating cells, include growth arrest in G_1 of the cell cycle, morphological and biochemical alterations in the cell surface leading to the mating-specific 'shmoo' morphology and transcriptional activation of genes whose products facilitate cellular and nuclear fusion (Herskowitz, 1995).

Some of the components of this signaling cascade are not only involved in mating but also in inducing morphological transitions of yeast cells. The switch to pseudohyphal and invasive growth requires Ste20p, Ste11p, Ste7p and Ste12p (Liu *et al.*, 1993; Roberts and Fink, 1994). The MAP kinases involved in this response are as yet unidentified (Liu *et al.*, 1993; Roberts and Fink, 1994).

Ste20p shares an essential function with the closely related isoform Cla4p in polarized cell growth during budding and cytokinesis (Cvrckova *et al.*, 1995). Both enzymes belong to the Ste20p/p65^{PAK} family of protein kinases believed to be involved in the regulation of conserved MAP kinase pathways conveying signals from the cell surface to the nucleus (Bagrodia *et al.*, 1995; Polverino *et al.*, 1995; Brown *et al.*, 1996; Frost *et al.*, 1996). Members of this protein kinase family bind the Rho-like small GTP binding proteins Cdc42 or Rac at a conserved binding site which includes a conserved sequence motif of 16 amino acids that appears to be sufficient for binding of Cdc42 or Rac (Burbelo *et al.*, 1995). This sequence motif is also present in the non-receptor tyrosine kinases p120^{ACK} from mammalian cells and DPR2 from *Drosophila*, the mixed lineage kinase (MLK) family of serine/threonine protein kinases and in numerous non-kinase proteins without defined biochemical activity, including WASP, a protein implicated in the immunodeficiency disorder Wiskott–Aldrich syndrome (Burbelo *et al.*, 1995).

In mammalian cells, Cdc42 and Rac regulate morphological responses such as membrane ruffling and the formation of filopodia in fibroblasts in response to numerous mitogenic stimuli (for a review, see Hall, 1994). It is now generally believed that at least some of these effects are mediated through kinases of the Ste20p/p65^{PAK}

family and the conserved c-Jun N-terminal kinase/stress-activated protein kinase (JNK/SAPK) pathway (Bagrodia *et al.*, 1995; Polverino *et al.*, 1995; Pombo *et al.*, 1995; Brown *et al.*, 1996; Frost *et al.*, 1996). Isoforms of $p65^{PAK}$ can be activated not only by small GTPases but also by heterotrimeric G-proteins in various signaling pathways (Knaus *et al.*, 1995; Teo *et al.*, 1995).

Yeast Cdc42p (Johnson and Pringle, 1990), its GDP–GTP exchange factor Cdc24p (Zheng *et al.*, 1994) and the SH3 domain protein Bem1p (Chenevert *et al.*, 1992), which associates with Cdc24p (Peterson *et al.*, 1994) and Ste20p (Leeuw *et al.*, 1995), are involved in controlling cell polarity during budding and in response to pheromone (for a review, see Chant and Stowers, 1995). Recent evidence suggests that Cdc42p and Cdc24p are also involved in pheromone signaling, and it has been proposed that the Cdc42p–GTPase cycle might play a role in linking Ste20p to the heterotrimeric mating response G-protein (Simon *et al.*, 1995; Zhao *et al.*, 1995). Moreover, Cdc42p has been shown to act upstream of Ste20p in the pathway that regulates filamentous growth (Mösch *et al.*, 1996).

Here, we show in a mutational analysis of Ste20p that the Cdc42p binding domain is dispensable for pheromone signaling. However, the Cdc42p binding domain is needed for cell–cell adhesion during conjugation, for morphological switching in response to a nutritional signal and for an essential function shared by Ste20p and Cla4p during vegetative growth. We also demonstrate that the Cdc42p binding domain is required to direct localization of Ste20p to the actin cytoskeleton in regions of polarized growth during budding. These results do not support the view that Ste20p acts as a mediator of Cdc42p in pheromone signaling, but are consistent with the model that Ste20p represents an essential target of Cdc42p during morphological switching and vegetative growth.

Results

Interaction of Cdc42p with Ste20p

Ste20p has a tripartite structure with a large non-catalytic region in the amino-terminal half, a kinase domain in the carboxy-terminal half and a short non-catalytic sequence carboxy-terminal to the kinase domain (Leberer *et al.*, 1992a). We used the two-hybrid system and an *in vitro* binding assay to confirm that Cdc42p binding to Ste20p is restricted to a short domain within the amino-terminal half. This domain is conserved among the members of the Ste20p protein kinase family and has been shown biochemically to bind Cdc42p in both $p65^{PAK}$ and Ste20p (Manser *et al.*, 1994; Simon *et al.*, 1995; Zhao *et al.*, 1995).

As summarized in Figure 1A, two-hybrid interactions of either wild-type Cdc42p or its activated G12V mutant version were only found with the non-catalytic, amino-terminal half of Ste20p, and these interactions were abolished by deleting a stretch of 36 amino acids between amino acid residues 333 and 370, corresponding to the conserved Cdc42p binding domain first identified in $p65^{PAK}$ (Manser *et al.*, 1994). We did not observe interactions with full-length Ste20p, corroborating our previous observations that protein fragments might reveal two-hybrid interactions not seen between full-length proteins (Leeuw *et al.*, 1995; Whiteway *et al.*, 1995).

We then used a resin binding assay to demonstrate that a Ste20p mutant in which the Cdc42p binding domain had been deleted was unable to bind Cdc42p. Cdc42p fused to maltose binding protein (MBP) was affinity purified from *Escherichia coli*, activated with GTPγS and analyzed for its ability to bind to fusions of wild-type Ste20p and the $Ste20p^{\Delta 334–369}$ mutant with glutathione *S*-transferase (GST) immobilized on glutathione–Sepharose beads. The results indicated that MBP–Cdc42p bound to wild-type Ste20p but not to its mutant version (Figure 1B).

Role of the Cdc42p binding domain of Ste20p during mating

To characterize the functional role of non-catalytic sequences in the amino-terminal half of Ste20p, we constructed several amino-terminal truncation mutants which were expressed under the control of the galactose-inducible *GAL1* promoter (Figure 2A). Cells expressing truncations of Ste20p up to amino acid residue 495 (ΔN221, ΔN355 and ΔN494) were not affected by their ability to mate with a *STE20* wild-type strain (Figure 2A). The induction of a pheromone-inducible reporter gene, *FUS1::lacZ*, and the pheromone-induced formation of mating-specific cell shapes, as indicated by the formation of 'shmoo' morphologies, were also normal (Figure 2A). Cells expressing a truncation of Ste20p up to residue 610 (ΔN609) were reduced in their mating efficiencies (Figure 2A). These cells were also reduced in *FUS1::lacZ* induction but produced typical mating-specific morphologies at normal frequencies in response to pheromone (Figure 2A). Western blot analysis indicated that these cells produced less mutant protein when compared with cells producing wild-type Ste20p or the ΔN494 mutant (data not shown). Thus, it is conceivable that decreases in mating efficiencies and *FUS1::lacZ* induction in these cells are caused by reduced mutant protein levels.

Basal levels of *FUS1::lacZ* expression were slightly increased in cells overexpressing the ΔN494 and ΔN609 truncation mutants (Figure 2A). These elevated levels were not observed in *ste4*-deleted cells and hence were dependent on the function of G_β (data not shown). Moreover, the truncation mutants failed to suppress defects in mating and *FUS1::lacZ* induction in *ste4*-deleted cells (data not shown).

To study further the function of the Cdc42p binding domain, we used homologous recombination to replace the wild-type *STE20* gene with mutant alleles in which the sequences between amino acid residues 333 and 370 (Δ*334–369*) or 257 and 583 (Δ*258–582*) were deleted, respectively (Figure 2B). As shown by immunoblot analyses (Figure 3A), the mutant proteins were expressed at wild-type levels. We investigated the *in vitro* protein kinase activity of the Δ334–369 mutant protein immunopurified from yeast cells. Autophosphorylation and the ability to phosphorylate myelin basic protein were unaffected by the deletion (Figure 3B).

Cells carrying the Δ*334–369* and Δ*258–582* alleles, respectively, mated at wild-type levels with *STE20* wild-type tester cells (Figure 2B). As indicated by the formation of clear zones in α-factor halo assays, these cells responded to pheromone with growth arrest at the same pheromone levels as wild-type cells (Figure 4). Moreover, pheromone

A

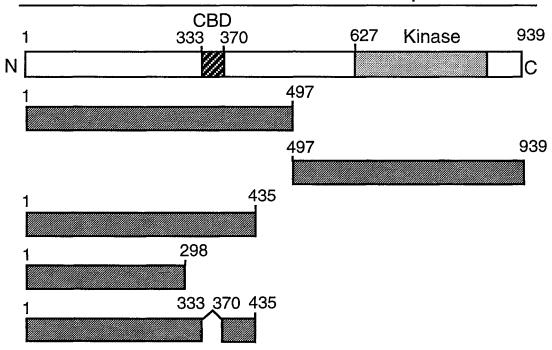

Gal4p-AD fusions with Cdc42p			
wild type		G12V	
β-Galactosidase activity	Growth on -His medium	β-Galactosidase activity	Growth on -His medium
0.09±0.01	-	0.08±0.02	-
1.19±0.11	+	1.18±0.31	+
0.11±0.01	-	0.13±0.02	-
4.18±0.12	+	2.32±0.52	+
0.11±0.01	-	0.12±0.01	-
0.06±0.01	-	0.08±0.03	-

B

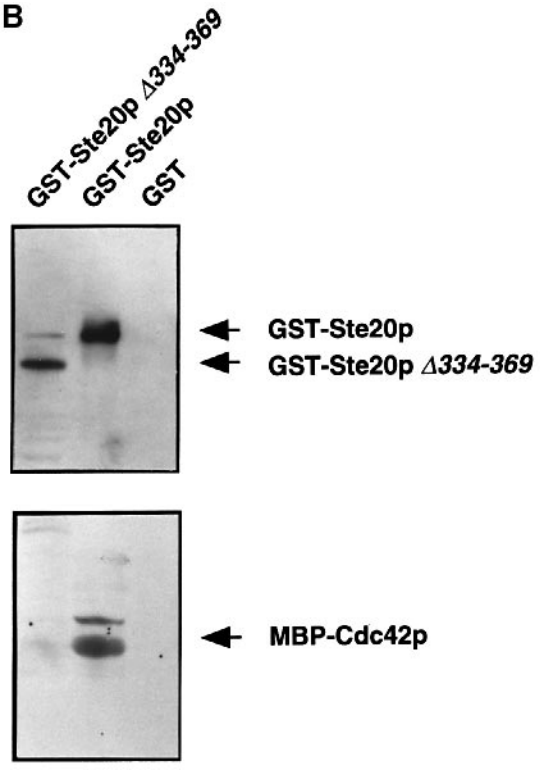

Fig. 1. Interactions of Ste20p with Cdc42p. (**A**) Two-hybrid interactions with wild-type Cdc42p and its activated G12V mutant version. Interactions were measured by using fusions with the DNA binding domain (DBD) of LexA and the transcriptional activation domain (AD) of Gal4p. Data (Miller units) are means ± SD of three independent experiments. Growth on –His medium was evaluated as (–) no growth, (+) normal growth. The Cdc42p binding domain (CBD) of Ste20p is indicated by the hatched bar. The plasmids were pDH37 ($Ste20p^{1–939}$), pRL27 ($Ste20p^{1–497}$), pRL7 ($Ste20p^{497–939}$), pAF3 ($Ste20p^{1–435}$), pAF2 ($Ste20p^{1–298}$), pRL99 ($Ste20p^{1–435/\Delta334–369}$), pRL39 (Cdc42p wild-type) and pRL58 ($Cdc42p^{G12V}$). All plasmids were also tested in combination with lamin fusion constructs as controls. These transformants did not grow on –His medium and had β-galactosidase activities of 0.05–0.11 units. (**B**) Resin binding assay to determine interactions between Ste20p and Cdc42p. GST–$Ste20p^{\Delta334–369}$, GST–Ste20p and GST were bound to glutathione–Sepharose beads and incubated with GTPγS-loaded Cdc42p fused to maltose binding protein (MBP). After washing, the beads were subjected to SDS–PAGE in 7.0% (upper panel) and 10.0% (lower panel) gels and immunoblotted for the presence of Ste20p–GST (upper panel) and Cdc42p–MBP (lower panel) with antibodies to Ste20p and MBP, respectively. GTPγS-loaded Cdc42p bound to wild-type Ste20p but not to its mutant version. No binding was observed with GDPβS-loaded Cdc42p (data not shown).

concentration-dependent *FUS1::lacZ* induction of mutant cells was indistinguishable from wild-type cells (Figure 5).

The mating efficiencies of cells carrying the Δ*334–369* and Δ*258–582* alleles, respectively, were reduced when the mating partner of the opposite mating type also carried the same allele (Table I). This bilateral defect is similar to *far1* mutant cells where mating is only attenuated slightly as long as one mating partner carries the *FAR1* wild-type gene but is reduced drastically when both mating partners carry *far1* mutations (Valtz *et al.*, 1995). This mating defect of *far1* mutant cells has been ascribed to a defect in oriented projection formation toward the mating partner (Dorer *et al.*, 1995; Valtz *et al.*, 1995).

Indeed, we found that cells carrying either the Δ*334–369* or Δ*258–582* alleles of *STE20* were defective in mating with *far1-c* mutant cells (Table I). We therefore investigated the possibility that cells carrying the *ste20* mutant alleles, like *far1-c* mutant cells, might be defective in oriented morphogenesis. We analyzed the *ste20* mutant cells in a direct microscope assay for orientation in a spatial gradient of α-factor (Segall, 1993). As illustrated in Figure 6, cells carrying the Δ*334–369* allele were able to produce projections growing in the direction of the tip of a pheromone-releasing micropipet. The degree of orientation was quantified by determining the cosine of the angle between the direction of projection formation

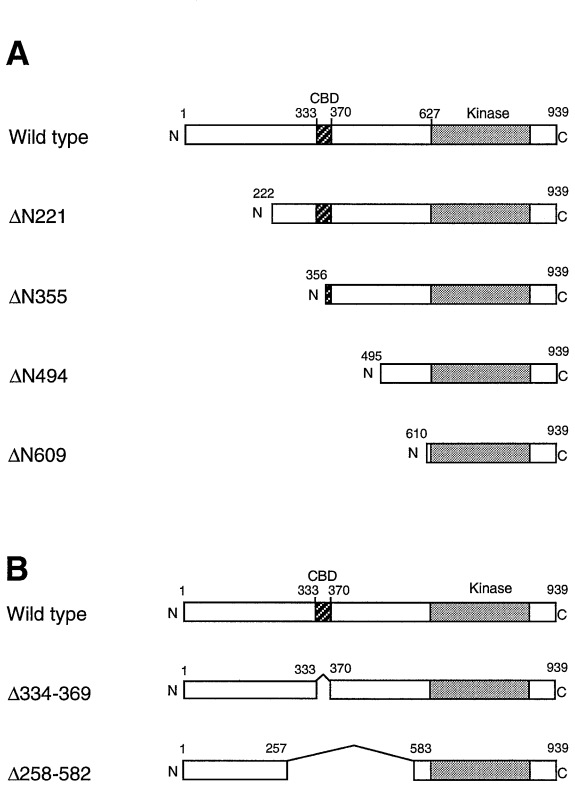

	Mating efficiency (%)	*FUS1::lacZ* expression		Shmoos (% of cells)
		Basal	Induced	
A				
Wild type	89.8 ± 15.5	0.1	221.2	89 ± 4
ΔN221	84.7 ± 6.7	< 0.1	180.9	92 ± 6
ΔN355	91.5 ± 5.4	< 0.1	210.3	88 ± 4
ΔN494	79.3 ± 14.8	2.7	153.4	83 ± 7
ΔN609	3.1 ± 0.7	1.3	7.4	75 ± 10
B				
Wild type	96.3 ± 3.2	4.0 ± 0.3	637.3 ± 34.0	88 ± 6
Δ334-369	92.3 ± 18.4	3.5 ± 2.7	517.3 ± 55.1	92 ± 7
Δ258-582	81.4 ± 19.1	4.3 ± 1.8	596.5 ± 63.2	86 ± 5

Fig. 2. Mating functions of Ste20p deletion mutants. (**A**) Wild-type Ste20p and amino-terminal truncation mutants were placed under control of the *GAL1* promoter and transformed into *ste20*-deleted cells (YEL206 to measure mating efficiencies, or supersensitive *sst1* YEL120 to measure shmoo formation and *FUS1::lacZ* induction). Cells were grown in selective (2%) raffinose medium to mid-exponential phase. Mating efficiencies were then determined in galactose (4%) medium at 30°C with the tester strain A281-4C (mean values ± SD of three independent experiments). To examine pheromone-induced shmoo formation, cells were switched to galactose (4%) medium containing 0.1 μM α-factor and grown for 6 h at 30°C. Cells were sonicated briefly and observed microscopically to determine cell shape. 'Shmoo' formation is given as percentage of cells producing one or more projections (means ± SD, $n = 3$; for each experiment, 200 cells were counted). To analyze *FUS1::lacZ* induction, cells were transformed with the reporter plasmid pSB234 and grown in selective raffinose (2%) medium to mid-exponential phase. After addition of 4% galactose, cells were incubated for 2 h at 30°C. Half of the cells were then treated with 0.1 μM α-factor for 6 h at 30°C and β-galactosidase activities were measured (expressed in Miller units). (**B**) Internal Ste20p deletion mutants were integrated into the genome. Mating efficiencies (strains YEL276 and YEL285 transformed with plasmid pRS313) were determined with the tester strain A-281-4C (mean values ± SD of three independent experiments). Pheromone-induced projection formation of the supersensitive strains YEL286 and YEL288 was examined microscopically as described above after 6 h of growth in YEPD medium containing 0.1 μM α-factor. Values are given as percentage of cells producing one or more projections (means ± SD, $n = 3$; for each experiment, 200 cells were counted). To analyze *FUS1::lacZ* induction, cells were transformed with the reporter plasmid pSB234 and grown in selective raffinose (2%) medium to mid-exponential phase. Half of the cells were then treated with 0.1 μM α-factor for 6 h at 30°C and β-galactosidase activity was measured (expressed in Miller units). In cells deleted for *STE20*, the mating efficiency was <0.00001%, basal and induced *FUS1::lacZ* expressions were <0.1 and projection formation was 0.

and the direction of the micropipet (Segall, 1993). Perfect orientation toward the pipet is indicated by a cosine of 1.0, random orientation by a cosine of 0 and perfect orientation away from the pipet by a cosine of –1.0. The *STE20* wild-type cells were found to orient with a cosine of 0.73 ± 0.029 ($n = 12$), whereas the *ste20* mutant cells oriented with a value of 0.73 ± 0.036 ($n = 23$). Similar values were obtained for cells carrying the $ste20^{\Delta 258–582}$ allele. These results indicate a high degree of orientation for both *STE20* wild-type and *ste20* mutant cells and exclude the possibility that mating defects between either *ste20* mutant cells or *ste20* and *far1* mutant cells are caused by defects in oriented morphogenesis.

The microscopic inspection of mating assay mixtures revealed the presence of a high percentage of zygotes when at least one mating partner carried wild-type genes of both *STE20* and *FAR1* (Table I). However, only few zygotes were found when mating was performed between two *ste20* mutant strains or between *ste20* and *far1* mutant strains (Table I). The percentage of cells producing projections was high in these mating mixtures (Table I). However, these projection-forming cells were not attached to each other. These results suggest that *ste20* mutant cells were able to respond morphologically to cells of opposite mating type but were defective in cell–cell adhesion and, therefore, unable to form zygotes when the opposite mating partner carried mutations in either *STE20* or *FAR1*.

Perturbation of the actin cytoskeleton by overexpression of amino-terminally truncated Ste20p mutant proteins

Galactose-induced overexpression of an amino-terminal truncation allele of *STE20* has been reported to be deleterious to growth (Ramer and Davis, 1993). We found that cells overexpressing the Δ*N221* or Δ*N355* alleles were viable (Figure 7A). In contrast, prolonged galactose-induced overexpression of either the Δ*N494* or Δ*N609* alleles was lethal (Figure 7A). This result was also obtained in cells deleted for either *STE4*, *STE5*, *FAR1* or *STE12*, or in diploid cells (data not shown), suggesting that

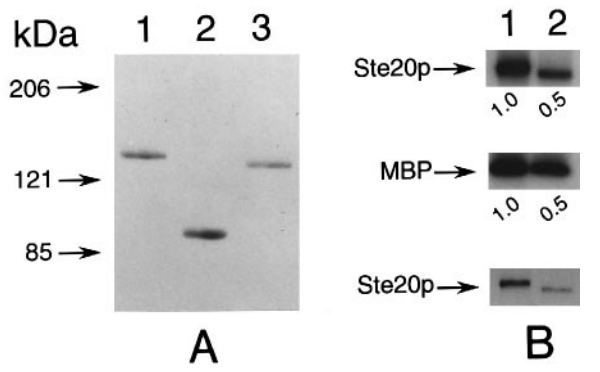

Fig. 3. Biochemical characterization of Ste20p deletion mutants. (**A**) Immunoblot analysis of extracts prepared from *STE20* wild-type (lane 1; strain W303-1A), *ste20*$^{\Delta 258–582}$ (lane 2; strain YEL285) and *ste20*$^{\Delta 334–369}$ (lane 3; strain YEL276) cells. (**B**) *In vitro* protein kinase activities of Ste20p in immune complexes isolated from *STE20* wild-type (lane 1) and *ste20*$^{\Delta 334–369}$ mutant (lane 2) cells. The immune complexes were analyzed for autophosphorylation (upper panel), myelin basic protein (MBP) phosphorylation (middle panel) and immunodetectable Ste20p protein (lower panel). The autoradiographs and immunoblots were analyzed densitometrically with a laser scanner. The relative phosphorylation levels were calculated in relation to the relative protein amounts and are shown on the bottom of the autoradiographs.

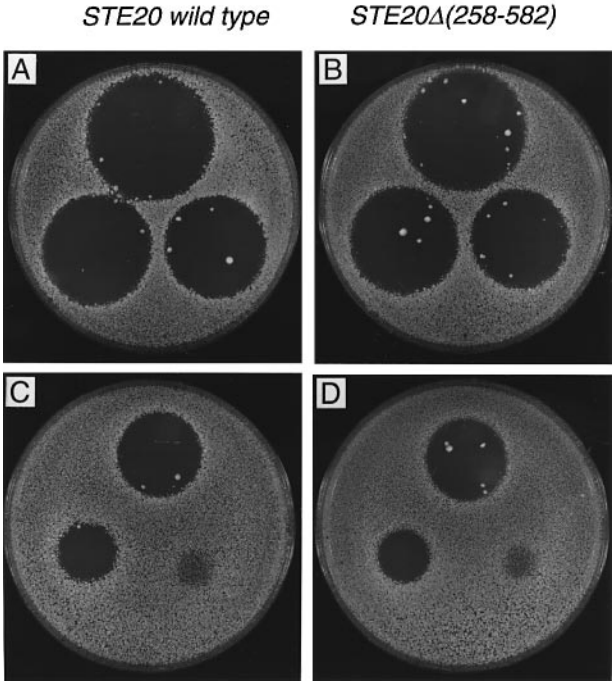

Fig. 4. Growth arrest assays of (**A**) and (**C**) *STE20* wild-type (supersensitive *sst1* strain YEL106) and (**B**) and (**D**) *ste20*$^{\Delta 258–582}$ mutant (supersensitive *sst1* strain YEL288) cells. Exponentially growing cells (10^6) were embedded into molten agar medium, and 50, 5 or 2 (A and B; counterclockwise from top) and 0.5, 0.05 or 0.005 μg (C and D; counterclockwise from top) of α-factor (solubilized in 5 μl of 90% methanol) were added onto the surface of the plates. Photographs were taken after 1 day of incubation at 30°C. Identical results were obtained with cells carrying the *ste20*$^{\Delta 334–369}$ allele (strain YEL286; data not shown).

lethality was not dependent on the pheromone response pathway.

The morphology of cells overexpressing the Δ*N494* or Δ*N609* alleles was enlarged and rounded (Figure 7B). Cell ghosts, indicative of cell lysis, could be observed after

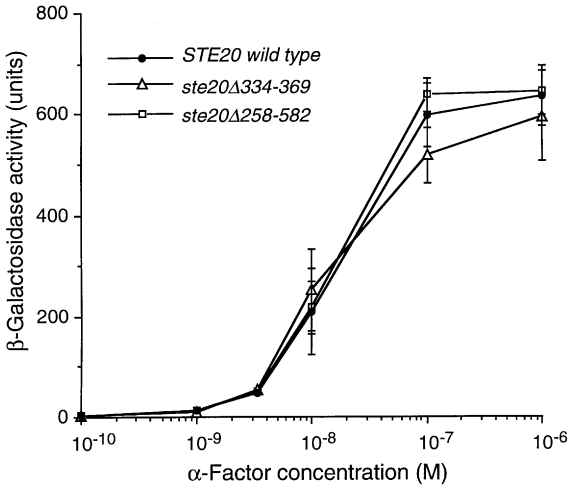

Fig. 5. Pheromone concentration dependence of *FUS1::lacZ* induction. The reporter plasmid pSB234 (Trueheart *et al.*, 1987) was introduced into isogenic supersensitive (*sst1*) *STE20* wild-type (strain YEL106), *ste20*$^{\Delta 334–369}$ mutant (strain YEL286) and *ste20*$^{\Delta 258–582}$ mutant (strain YEL288) cells. Transformants were grown in selective medium at 30°C to mid-exponential phase and then incubated for 6 h at 30°C with the indicated α-factor concentrations. β-Galactosidase activities were then measured and are given as mean values ± SD of three independent experiments.

prolonged expression (data not shown). Since we previously found that a fraction of Ste20p co-purified with actin (Leeuw *et al.*, 1995), we investigated whether the truncation mutants might interfere with the reorganization of the actin cytoskeleton during budding. Cells overproducing wild-type Ste20p showed normal actin staining with rhodamine–phalloidin (Figure 7B). In proliferating cells, actin was polarized toward the developing bud, and, in pheromone-induced cells, actin was polarized toward the 'shmoo' tip. Cells overproducing the Δ*N494* allele revealed an abnormal actin staining pattern with small patches distributed all over the cell (Figure 7B). However, pheromone treatment of these cells induced normal orientation of actin toward the 'shmoo' tips (Figure 7B). We conclude from these experiments that overexpression of truncated Ste20p mutants perturbs the polarized reorganization of the actin cytoskeleton during budding but not during the formation of mating-specific morphologies.

The Cdc42p binding domain of Ste20p is necessary for cellular viability in the absence of Cla4p

Ste20p and Cla4p share a redundant function that is essential for cellular viability (Cvrckova *et al.*, 1995). Cells deleted for *CLA4* alone are viable but have defects in cytokinesis (Cvrckova *et al.*, 1995). Deletions of both *CLA4* and *STE20* cause lethality (Cvrckova *et al.*, 1995). To examine whether the non-catalytic sequences of Ste20p, including the Cdc42p binding domain, are necessary for vegetative growth in the absence of Cla4p, we analyzed the various Ste20p mutants in a strain that was deleted for both *CLA4* and *STE20*.

Plasmids carrying the various amino-terminal *ste20* truncation mutants under control of the *GAL1* promoter were transformed into a *cla4*Δ *ste20*Δ strain whose viability was supported by a plasmid carrying *CLA4* and *URA3* as selectable marker. Expression of the *ste20* mutants was then induced by galactose, and loss of the *CLA4* plasmid

Table I. Mating and zygote formation defects of *ste20* mutant cells

Relevant genotypes		Mating efficiencies (%)	Zygotes (% of total cells)	Shmoos (% of total cells)
a cell	α cell			
STE20	*STE20*	90.2 ± 8.3	13	1
$ste20^{\Delta 334–369}$	*STE20*	85.1 ± 10.2	14	0.5
$ste20^{\Delta 258–582}$	*STE20*	88.2 ± 5.9	11	2
$ste20^{\Delta 334–369}$	$ste20^{\Delta 334–369}$	0.4 ± 0.2	<0.1	15
$ste20^{\Delta 258–582}$	$ste20^{\Delta 258–582}$	0.3 ± 0.1	0.1	12
STE20	*far1-c*	9.2 ± 0.5	1	13
$ste20^{\Delta 334–369}$	*far1-c*	0.3 ± 0.1	<0.1	16
$ste20^{\Delta 258–582}$	*far1-c*	0.5	<0.1	15

The strains used were W303-1A (*MAT***a** *STE20*), YEL276 (*MAT***a** $ste20^{\Delta 334–369}$), YEL285 (*MAT***a** $ste20^{\Delta 258–582}$), IH1793 (*MAT*α *STE20*), YEL324-1B (*MAT*α $ste20^{\Delta 334–369}$), YEL325-1B (*MAT*α $ste20^{\Delta 258–582}$) and JC31-7D (*MAT*α *far1-c*). Cells were grown at 30°C to mid-exponential phase. Mating was then determined by mixing 1×10^6 *MAT***a** cells with 5×10^6 *MAT*α cells and performing the filter mating assay at 30°C for 4 h. Data represent mean values ± SD of three independent experiments. To examine zygote and 'shmoo' formation, aliquots of mating mixtures were removed from the filters after 2 h and examined microscopically for the presence of zygotes and 'shmoos' (cells with one or more projections). For each sample, 1000 cells were counted and data were expressed as percentage of total cell number.

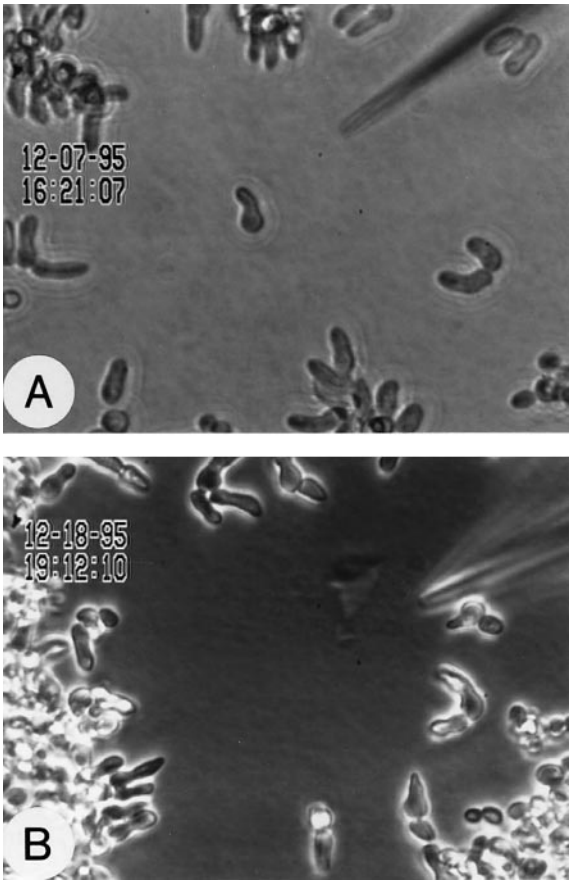

Fig. 6. Responses of (**A**) *STE20* wild-type (strain YEL106) and (**B**) $ste20^{\Delta 334–369}$ mutant (strainYEL286) cells in a spatial gradient of α-factor. Exponentially growing cells were analyzed with 67 nM α-factor in the pipet at 30°C. Images were taken 5 h after induction with pheromone. The out-of-focus micropipet is coming from the upper right corner and is directed to the center of the image.

was enforced by the presence of 5-fluoroorotic acid (Boeke *et al.*, 1987) (Figure 7A). Cells expressing the Δ*N221* allele of *STE20* were fully viable, whereas cells expressing the Δ*N355*, Δ*N494* or Δ*N609* alleles were unable to grow. A microscopic analysis of these cells showed a pleiotropic population of large and irregularly shaped cells and revealed many cell ghosts (data not shown). Thus, the amino-terminal region up to amino acid 222 was not essential for viability in the absence of Cla4p. However, the ability to support viability in the absence of Cla4p was lost after partial removal of the Cdc42p binding domain in the ΔN355 mutant.

To investigate further the role of the Cdc42p binding domain of Ste20p in vegetative growth, we constructed *cla4*Δ strains that were either deleted for genomic *STE20* or in which genomic *STE20* was replaced with the Δ*334–369* allele by homologous recombination. Viability of the double mutant cells was supported by galactose-induced expression of *CLA4* carried on a plasmid. *CLA4* expression was then suppressed by replica plating patches of yeast cells from galactose medium to glucose medium. As illustrated in Figure 8, Cla4p-depleted cells were viable when they carried the wild-type *STE20* gene but were unable to grow when they were completely deleted for *STE20* or when *STE20* was replaced with the Δ*334–369* allele. The microscopic inspection revealed a heterogeneous population of large and aberrantly shaped *cla4*Δ $ste20^{\Delta 334–369}$ cells that were similar to *cla4*Δ *ste20*Δ cells. These results indicate that the Cdc42p binding domain of Ste20p plays an essential role in vegetative growth in the absence of Cla4p.

Essential role of the Cdc42p binding domain of Ste20p in pseudomycelial growth

Ste20p is required for the induction of filamentous growth in response to nitrogen starvation (Liu *et al.*, 1993). To determine whether the non-catalytic region of Ste20p is necessary for this response, we transformed diploid cells deleted for both alleles of *STE20* with plasmids expressing the $ste20^{\Delta 334–369}$ and $ste20^{\Delta 258–582}$ alleles and induced the transformants by nitrogen starvation. As shown in Figure 9, transformants with the mutant alleles were unable to form pseudohyphae, although transformants expressing wild-type *STE20* were able to do so. These findings suggest that the Cdc42p binding domain of Ste20p is necessary for mediating the starvation signal.

The Cdc42p binding domain is required for subcellular localization of Ste20p

Finally, we asked whether the Cdc42p binding site is necessary for the subcellular localization of Ste20p. The sequence encoding green fluorescent protein (GFP)

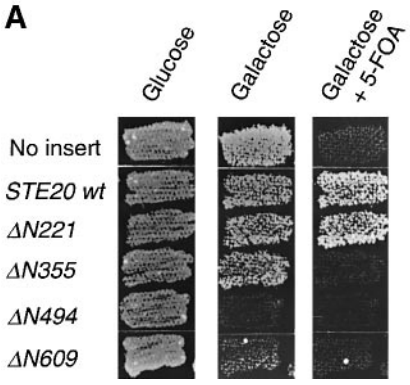

Fig. 7. Galactose-induced overexpression of amino-terminally truncated Ste20p mutants. (**A**) Effect of truncations on cellular viability and on the ability to complement *ste20 cla4* mutations. Cells deleted for both *STE20* and *CLA4* (strain YEL257-1A-1) contained plasmid pRL21 carrying *URA3* for selection and *CLA4* to support viability. These cells were transformed with pRS313GAL plasmids carrying *HIS3* as selectable marker and either no insert, wild-type *STE20* or the indicated truncation alleles under control of the *GAL1* promoter. Patches of transformants were grown on –His medium containing 2% glucose (left panel). Patches were then replica plated onto –His media containing either 4% galactose (middle panel) or 4% galactose and 0.1% 5-fluoroorotic acid (5-FOA; right panel), grown overnight at 30°C, replica plated again on the same media and grown for another day. Cells were forced by 5-FOA to lose the *CLA4* plasmid and were therefore dependent on the function of the *STE20* alleles to support viability. Galactose-induced expression of the Δ*N494* and Δ*N609* alleles was detrimental for viability. This effect was also seen in other strains including those that were wild-type for *STE20* or *CLA4* (data not shown). Expression of the Δ*N355* allele was unable to support viability in the absence of *CLA4*. (**B**) Effect of overexpression of the Δ*N494* allele of *STE20* on the actin cytoskeleton. Cells deleted for *STE20* (strain YEL206) were transformed with pRS313GAL plasmids carrying either the $ste20^{\Delta N494}$ allele or wild-type (wt) *STE20* under control of the *GAL1* promoter. Transformants were grown in selective raffinose (2%) medium to mid-exponential phase at 30°C. After addition of 4% galactose, cells were grown for 4 h in the absence or presence of 1 μM α-factor. Fixed cells were then stained with rhodamine–phalloidin to visualize actin. Photomicrographs of representative cells were then taken by Nomarski optics and rhodamine fluorescence with a 100× objective (bar = 5 μm). Similar effects on actin were seen in cells expressing the Δ*N609* allele of *STE20* (data not shown).

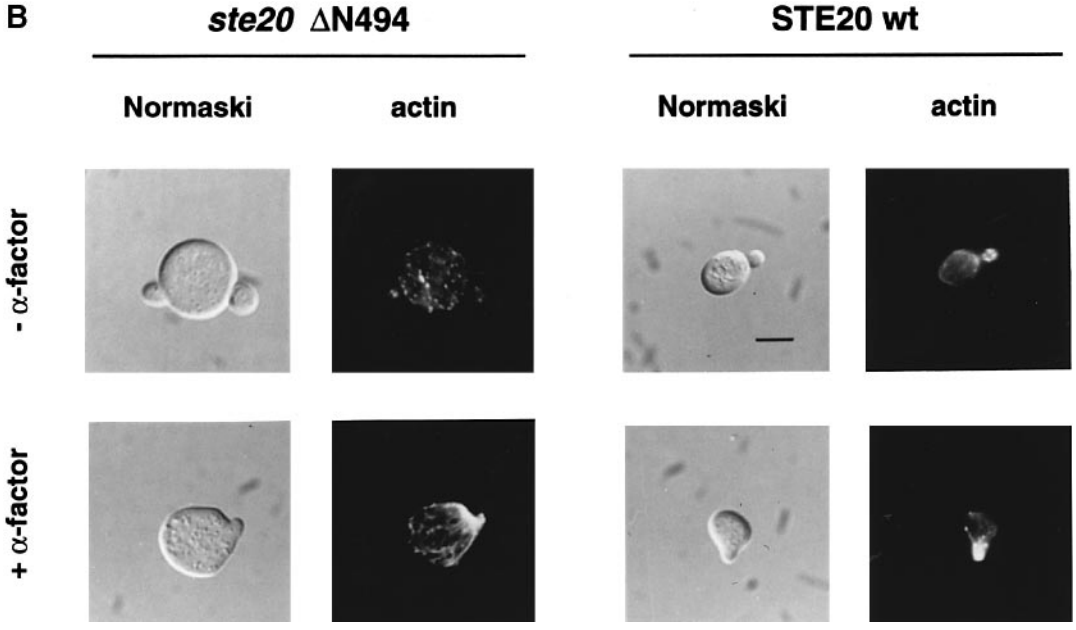

(Chalfie *et al.*, 1994) was fused to the amino-terminal sequence of *STE20* and the $ste20^{\Delta 334–369}$ allele. The chimeric proteins were fully functional, as shown by complementation of the mating defect of cells deleted for *STE20* (data not shown). Examination of cells deleted for *STE20* but expressing the GFP–Ste20p wild-type fusion protein under the *STE20* promoter on a centromere-based plasmid showed that the fusion protein localized at low concentrations to the plasma membrane and to cortical actin patches, and was concentrated in the growing bud (Figure 10b). This asymmetric distribution pattern was similar to the rhodamine–phalloidin staining pattern of actin (Figure 10c). GFP alone was found to be distributed uniformly in the cell (data not shown).

In pheromone-induced cells, the fusion protein was concentrated intracellularly in the ‘shmoo’ tip, giving rise to a crescent-like staining pattern (Figure 10e). Again, this asymmetric distribution pattern was similar to the rhodamine–phalloidin staining pattern of actin (Figure 10c and f).

Cells expressing the GFP–Ste20p$^{\Delta 334–369}$ fusion protein showed a normal pattern of actin staining during both budding and ‘shmooing’ (Figure 10i and l). However, the GFP–Ste20p$^{\Delta 334–369}$ fusion protein showed a uniform

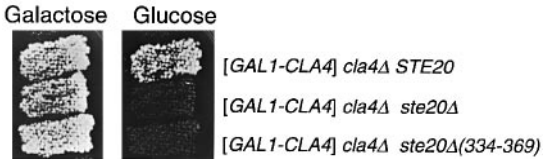

Fig. 8. Requirement of the Cdc42p binding site of Ste20p for cellular viability in the absence of Cla4p. Cells that were deleted for *CLA4* and carried either wild-type *STE20* (strain YEL257-12C), a deletion of *STE20* (strain YEL257-1A-2) or the *ste20*$^{\Delta 334–369}$ allele (strain YEL303-1B), contained plasmid pDH129 carrying *CLA4* under control of the *GAL1* promoter. Patches of cells were grown on selective galactose (4%) medium overnight at 30°C, then replica plated to selective glucose (2%) medium and grown for 24 h at 30°C. Viability of *cla4*Δ *ste20*Δ or *cla4*Δ *ste20*$^{\Delta 334–369}$ double mutant cells was supported by galactose-induced expression of *CLA4* but was prevented by glucose-dependent suppression of *CLA4*.

intracellular distribution in the budding cells (Figure 10h). In pheromone-induced cells, the mutant fusion protein was also distributed all over the cell but was found at slightly higher concentrations in the 'shmoo' tip (Figure 10k). Based on these observations, we conclude that the Cdc42p binding domain plays an important role in directing subcellular localization of Ste20p to sites of polarized growth.

Discussion

The Cdc42p binding domain of Ste20p is required for interaction with Cdc42p but not for in vitro kinase activity

Ste20p contains within its amino-terminal non-catalytic half, between amino acid residues 333 and 370, a sequence which is homologous to the Cdc42p binding sites of mammalian p65^{PAK} or p120^{ACK} (Manser *et al.*, 1993, 1994). The sequence LRISTPYNAKHIHHVGVD from amino acid residues 335–352 corresponds to a sequence motif known to be sufficient to bind Cdc42 or Rac in a variety of Cdc42/Rac binding proteins (Burbelo *et al.*, 1995).

Consistent with the view that the Cdc42p binding domain may be the only region of Ste20p to bind Cdc42p, mutational removal of the sequence between residues 333 and 370 prevented the interaction with Cdc42p *in vivo* and *in vitro*, as shown by the two-hybrid interaction system and by a resin binding assay, respectively (Figure 1). Although these results do not completely exclude the possibility that Cdc42p might bind under *in vivo* conditions to other regions of Ste20p not detected by these methods, the defects of the Ste20p truncation mutants in morphological switching and cytokinesis strongly argue, as discussed below, for the view that these mutants have lost the ability to bind Cdc42p.

Removal of the Cdc42p binding site blocked neither the ability of Ste20p to autophosphorylate nor to phosphorylate a generic substrate, myelin basic protein, in an *in vitro* kinase assay (Figure 3). We found, in contrast to a previous study (Simon *et al.*, 1995), that the *in vitro* kinase activity of Ste20p was not activated by addition of GTPγS-Cdc42p (data not shown). This failure of activation was also observed for the Ste20p mutant proteins, although we found, in agreement with previous studies (Manser *et al.*, 1994; Martin *et al.*, 1995) that a GST–p65^{PAK} fusion protein could be activated under the same conditions (data not shown). One possible explanation for the discrepancy with the results from Simon *et al.* (1995) might be that these authors purified recombinant GST–Ste20p from insect cells, whereas in our case the native protein was isolated from yeast cells and might have been already in an activated state.

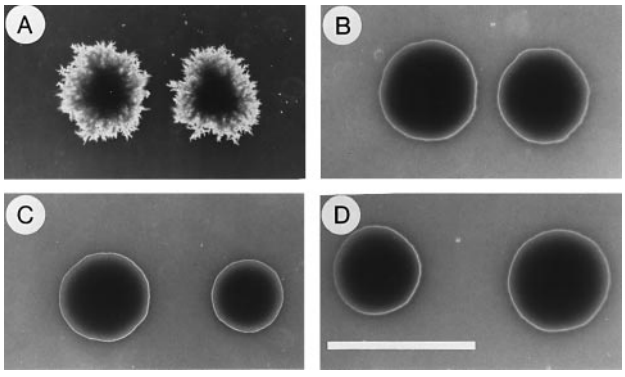

Fig. 9. Requirement of the Cdc42p binding site of Ste20p for pseudomycelial growth. The diploid *ste20/ste20* strain HLY492 was transformed with plasmids pSTE20-5 carrying wild-type *STE20* (**A**), pRS316 carrying no insert (**B**), pRS316-STE20(Δ334–369) carrying the *ste20*$^{\Delta 334–369}$ allele (**C**) and pRS316-STE20(Δ258–582) carrying the *ste20*$^{\Delta 258–582}$ allele (**D**), and colonies were grown on selective nitrogen starvation medium (Gimeno *et al.*, 1992) for 5 days at 30°C. Photomicrographs were taken with a 4× objective (bar = 1 mm).

Cdc42p binding to Ste20p is dispensable for pheromone signaling

Nearly all of the amino-terminal non-catalytic half of Ste20p (up to amino acid residue 583), including the Cdc42p binding site, could be removed without affecting mating-specific responses (Figures 2 and 4–6). Cdc42p binding-deficient Ste20p mutants were normally regulated in a pheromone-dependent manner *in vivo*. These findings contradict the view that Cdc42p binding to Ste20p provides a functional link between the Ste20p/MAP kinase module and the heterotrimeric G-protein (Simon *et al.*, 1995; Zhao *et al.*, 1995), and argue strongly for a direct regulation of Ste20p by the activated β- and γ-subunits of the mating response G-protein (Figure 11). This view is also supported by genetic interactions between *STE20* and *STE4* (encoding G_β) (Leberer *et al.*, 1992a) and our recent observation that G_β directly binds to Ste20p *in vivo* and *in vitro* (T.Leeuw and E.Leberer, unpublished results). Our results also imply that molecular determinants which specify the pheromone signaling function of Ste20p must lie within either the kinase domain or the non-catalytic sequence carboxy-terminal to the kinase domain. This conclusion is supported by findings that sequences carboxy-terminal to the kinase domain are essential for the mating function of Ste20p (E.Leberer, unpublished results). Activation of Ste20p may also involve the adaptor protein Ste5p (Figure 11) which has been shown to interact with the kinases of the MAP kinase module (for a review, see Elion, 1995), to co-immunoprecipitate with Ste20p (Leeuw *et al.*, 1995) and to associate directly with G_β (Whiteway *et al.*, 1995).

Cdc42p plays a role during mating. It is localized at both the bud site and the tips of mating projections and is required for the formation of these projections during mating (Johnson and Pringle, 1990; Ziman *et al.*, 1993). This function of Cdc42p is most likely under control of

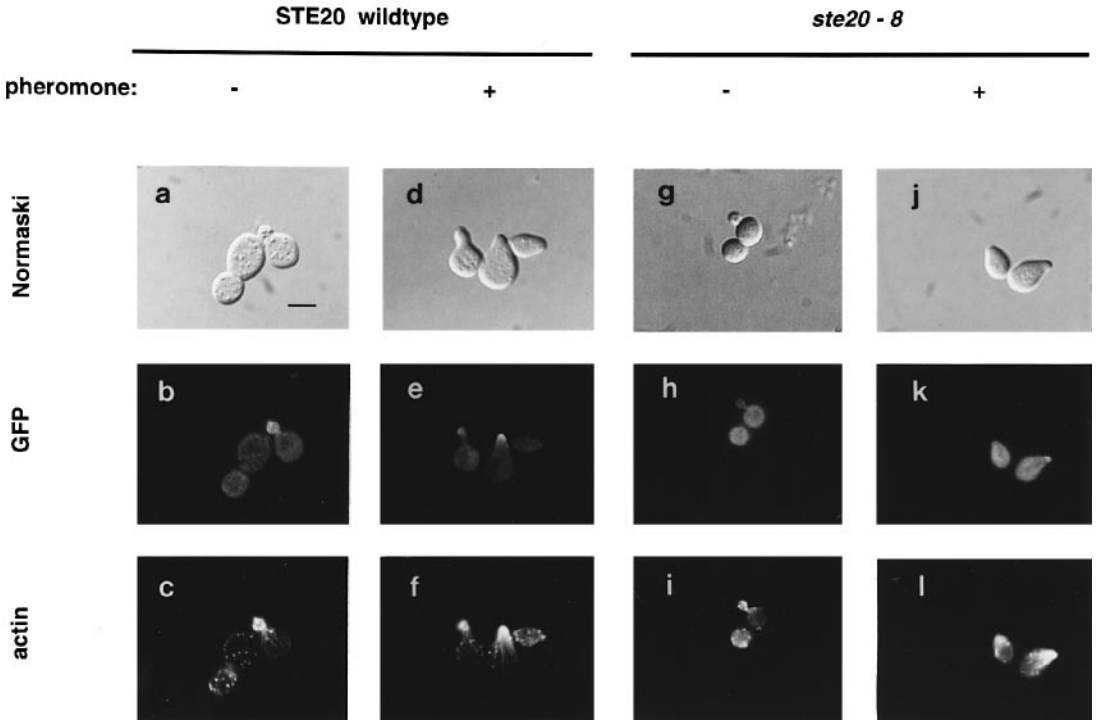

Fig. 10. Subcellular localization of GFP–Ste20p. Cells deleted for *STE20* (strain YEL206) were transformed with plasmids pRL116 and pBTL72 carrying fusions of GFP with wild-type *STE20* (**a**–**f**) and the *ste20*$^{\Delta 334-369}$ (*ste20-8*) allele (**g**–**l**), respectively. Transformants were grown in selective medium at room temperature to mid-exponential phase (a–c and g–i), and half of the cultures were incubated for 90 min with 1 μM α-factor at room temperature (d–f and j–l). Fixed cells were then stained with rhodamine–phalloidin, viewed by Nomarski optics (a, d, g and j) and analyzed for GFP fluorescence to visualize GFP–Ste20p chimeras (b, e, h and k) and rhodamine fluorescence to visualize actin (c, f, i and l). Identical distributions of GFP–Ste20p chimeras were observed in viable cells (data not shown). Photomicrographs were taken with a 100× objective (bar = 5 μm) and are representative for a large number of cells investigated.

the GDP–GTP exchange factor Cdc24p which binds to the β-subunit of the mating response G-protein (Zhao *et al.*, 1995). Temperature-sensitive mutations in *CDC42* and *CDC24* affect pheromone signaling (Simon *et al.*, 1995; Zhao *et al.*, 1995), and both overexpression of a constitutively activated form of Cdc42p (Simon *et al.*, 1995; Zhao *et al.*, 1995; Akada *et al.*, 1996) and deletion of *RGA1* encoding a putative GTPase-activating protein for Cdc42p (Stevenson *et al.*, 1995) weakly activate the pheromone response pathway. However, the data presented here suggest that any effects of Cdc42p on the pheromone signaling pathway and on pheromone-induced morphological changes are mediated by mechanisms that do not involve a physical interaction between Cdc42p and Ste20p (Figure 11). This conclusion is corroborated by the finding that overexpression of Cdc42p can improve mating in cells deleted for *STE20* (Leberer *et al.*, 1996).

Potential role of Cdc42p binding to Ste20p in cell–cell adhesion

A surprising result of this study was that Ste20p and Cdc42p might play roles in the initial phase of zygote formation when cells attach to each other (Figure 11). Although the formation of zygotes occurred at a normal frequency as long as one mating partner expressed wild-type Ste20p, zygote formation was reduced when both mating partners expressed Cdc42p binding-deficient Ste20p mutants (Table I). This bilateral mating defect is reminiscent of cells carrying mutations in the *FUS1*, *FUS2* or *FAR1* genes, where mating is nearly normal when at least one mating partner carries the corresponding wild-

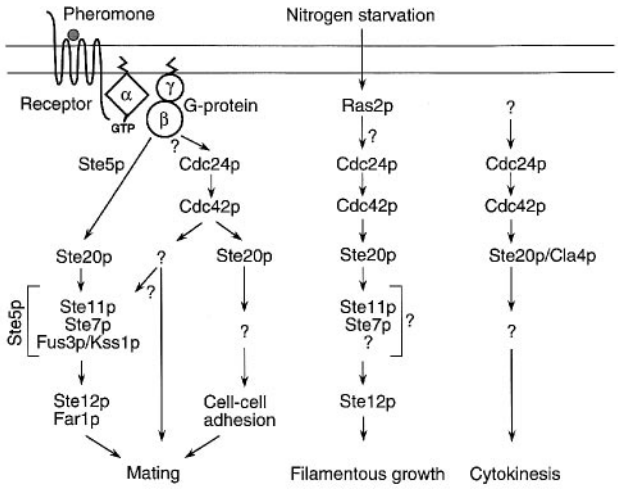

Fig. 11. Proposed model for multiple mechanisms of Ste20p regulation. Cdc42p binding to Ste20p is not required for activation of the pheromone-responsive MAP kinase pathway, but is essential for the induction of pseudohyphal growth and the control of polarized growth during budding. We propose that Ste20p is activated by $G_{\beta\gamma}$ during pheromone signaling by a mechanism that might involve the adaptor protein Ste5p which binds to G_{β} and the protein kinases acting downstream of Ste20p (Elion, 1995; Whiteway *et al.*, 1995). We also propose that Cdc42p is involved in pheromone signaling and mating through mechanisms that do not require binding to Ste20p. Our results suggest that Cdc42p binding to Ste20p plays a role in cell–cell adhesion during conjugation. In these pheromone-induced processes, Cdc42p is likely to be activated through its GDP–GTP exchange factor Cdc24p which has been shown to interact with G_{β} (Zhao *et al.*, 1995). Our model does not exclude the involvement of as yet unidentified components.

type gene, but is drastically attenuated when both mating partners carry mutations in these genes (McCaffrey *et al.*, 1987; Trueheart *et al.*, 1987; Dorer *et al.*, 1995; Elion *et al.*, 1995; Valtz *et al.*, 1995). However, in contrast to Cdc42p binding-deficient Ste20p mutant cells, *fus1* and *fus2* mutant cells are able to attach to each other but are delayed in cellular fusion (McCaffrey *et al.*, 1987; Trueheart *et al.*, 1987; Elion *et al.*, 1995). Interestingly, we also observed reduced mating and defective zygote formation when one mating partner expressed a Cdc42p binding-deficient Ste20p mutant and the opposite mating partner carried a *far1-c* mutant allele (Table I).

Cell–cell adhesion during zygote formation involves the combined effects of cell surface agglutinins (Lipke and Kurjan, 1992), orientation of a mating protrusion toward a neighboring cell with opposite mating type (Segall, 1993), a partner selection system (Jackson *et al.*, 1991) and the deposition of proteins required for the fusion of cells in the tips of the mating protrusions (McCaffrey *et al.*, 1987; Trueheart *et al.*, 1987; Elion *et al.*, 1995). The reduced mating efficiencies of Cdc42p binding-deficient Ste20p mutant cells could be explained if both mating partners are defective in orienting mating-specific protrusions toward the mating partner, a defect which has been ascribed to *far1-c* mutant cells (Dorer *et al.*, 1995; Valtz *et al.*, 1995). However, Cdc42p binding-deficient Ste20p mutant cells were able to respond morphologically to the mating partner by attaining a typical 'shmoo' morphology (Table I) and orienting mating protrusions toward the pheromone source (Figure 6).

A more likely interpretation assumes that Cdc42p binding to Ste20p plays a role in polarized transport of components required for cell–cell adhesion in the tips of mating projections. It is tempting to speculate that Cdc42p binding to Ste20p might provide a link between the pheromone signaling pathway and the Pkc1p/Mpk1p pathway which is stimulated in response to pheromone through Ste20p (Zarzov *et al.*, 1996). It has been speculated that this stimulation might be necessary for polarized cell wall synthesis during the formation of mating protrusions (Zarzov *et al.*, 1996). Interestingly, in mammalian cells, the Rho family members Cdc42, Rac1 and RhoA induce the formation of focal complexes, filopodia and lamellipodia which might be involved in cell attachment and hence functionally equivalent to mating protrusions (Kozma *et al.*, 1995; Nobes and Hall, 1995). Moreover, the Ste20p homolog of *Drosophila* has been shown recently to localize to focal adhesions in epidermal cells (Harden *et al.*, 1996). More research will be required to study further the roles of Ste20p and Cdc42p in cell–cell adhesion and zygote formation during conjugation.

Cdc42p binding to Ste20p is required to induce filamentous growth

Removal of the Cdc42p binding domain of Ste20p completely prevented the induction of pseudomycelial growth of diploid cells in response to nitrogen starvation (Figure 9). Moreover, haploid cells expressing a Cdc42p binding-deficient Ste20p mutant have been shown to be blocked in invasive growth (M.Peter, personal communication). These results are consistent with the recent demonstration that Cdc42p acts as a regulator of the pseudohyphal Ste20p/MAP kinase pathway which does not require the function of the heterotrimeric G-protein but involves the Ras homolog Ras2p (Mösch *et al.*, 1996). Thus, differential regulation of Ste20p by $G_{\beta\gamma}$ in response to pheromone and by GTP-Cdc42p in response to a nutritional signal might explain how the same protein kinase can regulate different developmental pathways within the same cell (Figure 11).

The Cdc42p binding domain of Ste20p is indispensable for vegetative growth in the absence of Cla4p

Ste20p and its isoform Cla4p share an as yet undefined essential role in vegetative growth (Cvrckova *et al.*, 1995). Both protein kinases are necessary for cytokinesis, proper formation of the septin ring and proper localization of cell surface growth with respect to the septin ring (Cvrckova *et al.*, 1995). Deletion of both genes, *CLA4* and *STE20*, causes lethality (Cvrckova *et al.*, 1995). This phenotype was not rescued by Cdc42p binding-deficient Ste20p mutants, indicating that the essential function of Ste20p requires Cdc42p binding (Figures 7A and 8). This result strongly suggests that Ste20p and Cla4p are essential targets of Cdc42p during vegetative growth (Figure 11). A role for Ste20p downstream of Cdc42p during budding is also suggested by the finding that multiple copies of *STE20* cure the growth defect of temperature-sensitive *cdc42* mutant cells at the restrictive temperature (Leberer *et al.*, 1996).

The Cdc42p binding domain is needed for proper intracellular localization of Ste20p

We have used fusions with GFP to determine the subcellular localization of Ste20p (Figure 10). As will be described elsewhere in more detail, GFP–Ste20p showed a cell cycle-dependent intracellular distribution. In G_1 of the cell cycle or in late mitosis, GFP–Ste20p localized to the plasma membrane and to cortical actin patches. In cells undergoing budding, GFP–Ste20p was accumulated in the growing bud together with cortical actin bundles (Figure 10b and c) and at the mother-bud neck in late mitosis (data not shown). This asymmetric distribution was lost after removal of the Cdc42p binding site although the polarized actin staining pattern remained unaffected (Figure 10h and i).

In pheromone-induced cells, GFP–Ste20p was concentrated with cortical actin bundles at the tips of mating protrusions, giving rise to a crescent-like staining pattern (Figure 10e and f). This kind of staining pattern has also been observed for Cdc42p (Ziman *et al.*, 1993). After removal of the Cdc42p binding site, Ste20p was distributed all over the cell but was still found at slightly higher concentrations in the projection tips where cortical actin bundles were oriented normally (Figure 10k and l). These results argue strongly for a role for Cdc42p in localizing Ste20p to regions of polarized growth where cortical actin bundles reorient, and are in agreement with our previous findings that a fraction of Ste20p co-purified with actin in sucrose density gradients (Leeuw *et al.*, 1995). Interestingly, Cdc42 binding to WASP, a protein implicated in the immunodeficiency disorder Wiskott–Aldrich syndrome, has been shown to direct localization of WASP to clusters of polymerized actin (Symons *et al.*, 1996).

Overexpression of truncated Ste20p mutants

Overexpression of the Δ*N494* and Δ*N609* alleles of *STE20* was deleterious to growth (Figure 7A) probably by preventing the normal reorientation of cortical actin into the emerging bud (Figure 7B). This lethality could be explained if the truncation mutants interfere with the functions of Ste20p and Cla4p during bud emergence, e.g. by preventing phosphorylation of a common substrate that regulates actin reorganization. Alternatively, the truncation mutants might be hyperactive and therefore phosphorylate substrates in an uncoordinated mode. Interestingly, destruction of the Cdc42p binding site was not sufficient to generate this lethal effect since overexpression of the ΔN355 (Figure 7A) and Δ334–369 (data not shown) mutant proteins, in which the conserved Cdc42p binding motif from amino acid residues 335–352 had been removed, was not detrimental (Figure 7A). Thus, to generate a deleterious truncation mutant, additional removal of sequences carboxy-terminal to the Cdc42p binding motif was required.

Overexpression of the ΔN494 and ΔN609 truncation mutants stimulated basal *FUS1::lacZ* expression (Figure 2A). This stimulation required the function of G_β (encoded by *STE4*), suggesting that a regulatory input from the heterotrimeric G-protein is required. Moreover, the truncation mutants did not complement the pheromone signaling defects in *ste4* mutant cells (data not shown). Stimulation of basal *FUS1::lacZ* expression was not observed in cells overexpressing the ΔN355 (Figure 2A) and Δ334–369 (data not shown) mutants, suggesting that additional removal of sequences carboxy-terminal to the conserved Cdc42p binding motif is required to engender this phenotype. We found that removal of these sequences did not affect the *in vitro* kinase activity of Ste20p (data not shown). However, stimulation of basal pheromone signaling by the ΔN494 and ΔN609 truncation mutants could be explained if removal of amino-terminal sequences improves the *in vivo* stimulation of Ste11p, which has been shown to be a substrate of Ste20p *in vitro* (Wu *et al.*, 1995).

Multiple mechanisms of Ste20p regulation

Taken together, our results demonstrate that Ste20p is regulated by multiple mechanisms during different developmental pathways (Figure 11). Cdc42p-dependent mechanisms are involved in morphological switching and the control of polarized growth and cytokinesis during cell proliferation, whereas a Cdc42p-independent mechanism is involved in G-protein-coupled receptor signaling. The high degree of conservation of the Ste20p/$p65^{PAK}$ family protein kinases suggests that similar multiple regulatory mechanisms may exist in other organisms including mammalian cells. It is conceivable that Cdc42/Rac-dependent and -independent mechanisms regulate mammalian $p65^{PAK}$ isoforms in different signaling pathways, and some of these mechanisms may depend on heterotrimeric G-proteins. Interestingly, some members of the Ste20p/$p65^{PAK}$ family are lacking a Cdc42/Rac binding site, including GC kinase which, like $p65^{PAK}$, is able to activate the JNK/SAPK pathway (Pombo *et al.*, 1995). Thus the same MAP kinase cascade may be regulated by Cdc42/Rac-dependent and -independent members of the same protein kinase family. An interplay with heterotrimeric and small G-proteins may provide a sensitive mode for fine tuning specificity of Ste20p/$p65^{PAK}$ protein kinases in various signaling pathways.

Materials and methods

Materials

Restriction endonucleases and DNA-modifying enzymes were obtained from Boehringer Mannheim, Bethesda Research Laboratories, Pharmacia LKB Biotechnology Inc. and New England Biolabs Inc. *Ultima Taq* thermostable DNA polymerase was purchased from Perkin Elmer. [γ-^{32}P]ATP was obtained from ICN. GTPγS and GDPβS were from Boehringer Mannheim. Rhodamine-labeled phalloidin was obtained from Molecular Probes. Glutathione–Sepharose beads and glutathione were obtained from Pharmacia Biotech Inc. Amylose–agarose beads and antibodies to maltose binding protein were purchased from New England Biolabs Inc. Synthetic α-factor was purchased from Sigma, dissolved in 90% methanol at a concentration of 10 mg/ml and stored at –20°C. Horseradish peroxidase-conjugated goat anti-rabbit IgG was obtained from Bio-Rad. All other reagents were of the highest purity grade commercially available.

Yeast manipulations

Yeast media, culture conditions and manipulations of yeast strains were as described (Rose *et al.*, 1990). Yeast transformations with circular or linearized plasmid DNA were carried out after treatment of yeast cells with lithium acetate (Rose *et al.*, 1990). Gene disruptions were performed by the one-step gene replacement method (Rose *et al.*, 1990).

Construction of plasmids

Plasmid pRS316-STE20 is a centromere *E.coli*–yeast shuttle vector containing *URA3* for selection in *S.cerevisiae* (Sikorski and Hieter, 1989) and the *STE20* gene (Leberer *et al.*, 1992a). Plasmid pVTU-STE20 is pVTU102-U carrying *STE20* under control of the *ADH1* promoter and *URA3* as selectable marker (Leberer *et al.*, 1992a).

To construct plasmid pVTU-STE20(Δ334–369), a fragment encoding the Cdc42p binding domain of Ste20p from amino acids 334 to 369 was removed by site-directed mutagenesis (Kunkel *et al.*, 1987) using single-stranded pVTU-STE20 as template and the oligodeoxynucleotide 5′-TCCTCATCTTCTATAACCACCACTTCTAGTGGTATTTCCAAAAG-3′ as primer. Plasmid pRS316-STE20(Δ334–369) was then constructed by replacing the *Bam*HI–*Xho*I fragment of plasmid pRS316-STE20 with the *Bam*HI– *Xho*I fragment of pVTU-STE20(Δ334–369). Plasmid pRS316-STE20(Δ258–582) was obtained by deleting the *Hin*dIII fragment from nucleotide positions 771–1746 of *STE20* from pRS316-STE20.

Plasmids carrying full-length and truncated versions of *STE20* under control of the *GAL1* promoter were constructed by cloning PCR (Saiki *et al.*, 1988) fragments of *STE20* into the *Spe*I and *Sac*II sites of plasmid pRS313GAL (Leberer *et al.*, 1992a). Plasmid pSTE20-5 (Leberer *et al.*, 1992a) was used as a template. *Ultima Taq* thermostable DNA polymerase was used in all PCR reactions. To construct plasmid pDH166 carrying full-length *STE20*, the oligodeoxynucleotide primers 5′-GACTAGTC-ATGAGCAATGATCCATCTGCT-3′ (ODH72) and 5′-TCCCCGCGGC-GATAATAAGGTGTACCCTGC-3′ (ODH76; the newly created *Spe*I and *Sac*II sites, respectively, are underlined) were used. The Δ*N221*, Δ*N355*, Δ*N494* and Δ*N609* truncation fragments were amplified by using the reverse primer ODH76 and the following forward primers (the newly created *Spe*I sites are underlined): 5′-GACTAGTCATGATCAATTC-AGCTTCCCATTCG-3′ (ODH81), 5′-GACTAGTCATGGGTGAGTA-CACAGGTTTGCCG-3′ (ODH73), 5′-GACTAGTCATGAATTCTG-CCGCCAATGTT-3′ (ODH74), and 5′-GACTAGTCATGATTTGCTCA-GACGGTGACCCA-3′ (ODH75).

To construct fusions of *STE20* with the cDNA encoding the S65T mutant version of GFP (Heim *et al.*, 1995), a *Bam*HI–*Spe*I fragment of the GFP cDNA was amplified by PCR using the oligodeoxynucleotides 5′-CGGGATCCGCTAGCATGAGTAAAGGAGAAGAAC-3′ and 5′-GGACTAGTTTGTATAGTTCATCCATGCC-3′ (the newly created *Bam*HI and *Spe*I sites, respectively, are underlined) as primers, and pRSET-S65T (kindly provided by R.Y.Tsien) as a template. The fragment was cloned into pRS316GAL (plasmid pRS316 carrying an *Eco*RI–*Bam*HI fragment of the *GAL1* promoter; Leberer *et al.*, 1992b) to create plasmid pBTL41. Plasmid pBTL72 carrying an in-frame fusion of the GFP–S65T cDNA with the amino-terminal sequence of full-length *STE20* was then constructed by cloning a *Spe*I–*Sac*II fragment of *STE20* (obtained from plasmid pDH166) into the respective sites of pBTL41.

Table II. Yeast strains

Strain	Genotype	Source or reference
W303-1A	*MAT***a** *ade2 his3 leu2 trp1 ura3 can1*	R.Rothstein
W303-1B	*MAT*α *ade2 his3 leu2 trp1 ura3 can1*	R.Rothstein
YEL106	W303-1A *sst1::LEU2*	Leberer *et al*. (1992b)
YEL120	W303-1A *sst1::LEU2 ste20-1::TRP1*	Leberer *et al*. (1992a)
YEL206	W303-1A *ste20-3*Δ*::TRP1*	Wu *et al*. (1995)
YEL276	W303-1A *ste20*$^{\Delta 334–369}$	this study
YEL285	W303-1A *ste20*$^{\Delta 258–582}$	this study
YEL286	W303-1A *sst1::LEU2 ste20*$^{\Delta 334–369}$	this study
YEL288	W303-1A *sst1::LEU2 ste20*$^{\Delta 258–582}$	this study
IH1793	*MAT*α *lys1*	Chenevert *et al*. (1994)
YEL324-1B	IH1793 *ste20*$^{\Delta 334–369}$	this study
YEL325-1B	IH1793 *ste20*$^{\Delta 258–582}$	this study
JC31-7D	IH1793 *far1-c*	Chenevert *et al*. (1994)
YEL257-12C	W303-1B *cla4*Δ*::TRP1* [pDH129::*HIS3*]	this study
YEL257-1A-1	W303-1B *ste20-3*Δ*::TRP1 cla4*Δ*::TRP1* [pRL21::*URA3*]	this study
YEL257-1A-2	W303-1B *ste20-3*Δ*::TRP1 cla4*Δ*::TRP1* [pDH129::*HIS3*]	this study
YEL303-1B	W303-1B *ste20*$^{\Delta 334–369}$ *cla4*Δ*::TRP1* [pDH129::*HIS3*]	this study
HLY492	*MAT***a**/α *ura3/ura3 ste20::TRP1/ste20::TRP1*	Liu *et al*. (1993)
M364-2C	*MAT***a** *his3 leu2 trp1 far1-1 LYS2::lexA-HIS3 URA3::lexA-lacZ*	Leeuw *et al*. (1995)
A281-4C	*MAT*α *his3*	A.Murray

To construct plasmid pBTL73 carrying an in-frame fusion of the GFP–S65T cDNA with the amino-terminal sequence of the *ste20*$^{\Delta 334–369}$ mutant allele, a *Spe*I–*Sac*II fragment of *ste20*$^{\Delta 334–369}$ was amplified by PCR using the oligodeoxynucleotides 5′-GACTAGTCATGAGCAATG-ATCCATCTGCT-3′ and 5′-TCCCCGCGGTTACCCGGGCTTTTGT-TTATCATCTTC-3′ as primers (the newly created *Spe*I and *Sac*II sites, respectively, are underlined) and pRS316-STE20(Δ334–369) as a template, and subsequently subcloned into pBTL41. Plasmids pRL116 and pBTL56, carrying the *GFP::STE20* chimeras under control of the *STE20* promoter, were then created by replacing the *GAL1* promoter in plasmids pBTL72 and pBTL73, respectively, with the *STE20* promotor amplified by PCR using the deoxynucleotides 5′-CCGCTCGAGGAATT-CTATCCAGAACCGCCT-3′ and 5′-GTTGCTAGCTTCTTGTATTAGT-CGAGGATC-3′ as primers (the newly created *Xho*I and *Nhe*I sites, respectively, are underlined) and plasmid pSTE20-5 as a template. These plasmids were found to fully complement the mating defect of cells deleted for *STE20* (data not shown).

Plasmid pRL21 is the yeast multicopy shuttle vector pRS426 (Christianson *et al.*, 1992) carrying the *CLA4* gene in a *Hin*dIII–*Eco*RI fragment (isolated from plasmid pC2537; Cvrckova *et al.*, 1995) and *URA3* as selectable marker. Plasmid pDH129 is pRS313GAL carrying *CLA4* under control of the *GAL1* promoter. To construct this plasmid, a *Xba*I–*Sac*II fragment of *CLA4* was amplified by PCR using the oligodeoxynucleotides 5′-GCTCTAGAGCATGTCTCTTTCAGCTG-CAGCG-3′ and 5′-TCCCCGCGGAATAGTTGTGTGCTTCATTCC-3′ (the newly created *Xba*I and *Sac*II sites, respectively, are underlined) as primers, and plasmid pC2537 as a template, and subcloned behind the *GAL1* promoter into pRS313GAL.

Yeast strains

The *S.cerevisiae* yeast strains used in this study are listed in Table II. Strains containing the *ste20*$^{\Delta 334–369}$ and *ste20*$^{\Delta 258–582}$ mutant alleles were constructed by a two-step procedure. The *Sph*I–*Xho*I fragments of plasmids pRS316-STE20(Δ334–369) and pRS316-STE20(Δ258–582) were subcloned into the integrating plasmid pRS306 (Sikorski and Hieter, 1989). The resulting plasmids were then linearized with *Bam*HI, transformed into strain W303-1A and *URA3*$^{+}$ transformants were selected. Subsequently *ura3*$^{-}$ derivatives were selected by growth in the presence of 5-fluoroorotic acid (Boeke *et al.*, 1987), and colonies that had become simultaneously *ura3*$^{-}$ and mating defective with the *MAT*α *far1-c* strain JC31-7D were selected. To ensure that wild-type *STE20* was replaced with the mutant versions, the *STE20* region was amplified by PCR using the oligodeoxynucleotides 5′-GCTGCCCATGAAGCTG-GTGGA-3′ and 5′-TACTTGGGTCACCGTCTGAGC-3′ as primers. Wild-type *STE20* produced a 1.7 kb fragment, whereas the mutant versions produced fragments of 1.6 and 1.3 kb in size, respectively.

Replacement of the sequence of the *CLA4* gene encoding the catalytic domain of Cla4p with *TRP1* was achieved as follows. The *Hin*dIII–*Eco*RI fragment of pC2537 (Cvrckova *et al.*, 1995) was subcloned into the Bluescript KS(+) vector (Stratagene) to yield plasmid pDH122. The *Nsi*I fragment from nucleotide positions 1084–2596 of the *CLA4* gene (Cvrckova *et al.*, 1995) was then replaced with a 0.9 kb *Pst*I–*Pst*I fragment derived from plasmid pJJ246 (Jones and Prakash, 1990) to yield plasmid pDH124. This plasmid was linearized with *Sma*I and *Kpn*I and transformed into yeast to replace 1.5 kb of the chromosomal *CLA4* gene with *TRP1* by homologous recombination (Rose *et al.*, 1990). The replacement was confirmed by PCR using oligodeoxynucleotide primers corresponding to the nucleotide sequences from positions 1012–1032 and 2742–2762 of the *CLA4* gene (Cvrckova *et al.*, 1995) (data not shown).

Yeast mating and orientation assays

Patch mating tests were carried out as described (Leberer *et al.*, 1992b). Quantitative mating assays were performed by a filter mating assay (Leberer *et al.*, 1993). Briefly, exponentially growing experimental cells were mixed with a 4-fold excess of exponentially growing tester cells and filtered through nitrocellulose filters. The filters were placed onto YEP-glucose (2%) or YEP-galactose (4%) plates and mating was allowed to proceed for 4 h at 30°C. The cells were then washed off the filters and titered on selective media to determine the number of diploid cells and the number of diploid cells plus experimental haploid cells. The mating efficiency was defined as the number of diploid cells determined on the first selective medium divided by the number of diploid plus experimental haploid cells determined on the second selective medium.

Orientation of yeast cells in a gradient of α-factor was measured as described (Segall, 1993).

Two-hybrid protein interaction assays

The assays were performed as described (Leeuw *et al.*, 1995) in strain M364-2C which is a *far1-1* derivative strain of L40. Plasmids pRL39 and pRL58 encoding fusions of the transciptional activation domain of Gal4p with the amino-terminus of Cdc42p and Cdc42p^{G12V}, respectively, were constructed by cloning PCR fragments into plasmid pGAD424 (Chien *et al.*, 1991). Wild-type *CDC42* was amplified by using the oligodeoxynucleotide primers 5′-CCGGAATTCATGCAAACGCTAAA-GTGTGTT-3′ (ORL9) and 5′-CGCGGATCCCTACAAAATTGTACAT-TTTTTACT-3′ (ORL10; the newly created *Eco*RI and *Bam*HI sites, respectively, are underlined) and plasmid pGAL-CDC42 (Ziman *et al.*, 1991) as a template. *CDC42*^{G12V} was amplified by using the oligodeoxy-nucleotide primers 5′-CCGGAATTCATGCAAACGCTAAAGTGTGT-TGTTGTCGT-3′ (ORL14; the newly created *Eco*RI site is underlined) and ORL10, and plasmid pGAL-CDC42^{G12V} (Ziman *et al.*, 1991) as a template. Plasmids encoding fusions of the LexA DNA binding domain with the amino-terminus of Ste20p fragments were constructed by cloning PCR fragments of *STE20* into plasmid pBTM116 (Chien *et al.*, 1991). Plasmid pDH37 encoding a full-length Ste20p fusion was constructed by amplifying a *Bgl*II–*Xho*I fragment of *STE20* as described (Leberer *et al.*, 1992a), and cloning this fragment into the *Bam*HI and *Sal*I sites of pBTM116. A 1.5 kb *Eco*RI fragment of this plasmid was then cloned into the *Eco*RI site of pBTM116 to create plasmid pRL27

encoding a Ste20p$^{1–497}$ fusion. Plasmid pRL7 encoding a Ste20p$^{497–939}$ fusion was made by amplifying a *Bam*HI–*Xho*I fragment of *STE20* using the oligodeoxynucleotide primers 5′-CGGGATCCTGAATTCTGCC-GCCAATGTTTC-3′ (OAF7; the *Bam*HI site used for cloning is underlined) and 5′-CCGCCGCTCGAGCTATCTTAGTGTACCACTATTTGA-3′ (OAF1; the newly created *Xho*I site is underlined), and pDH37 as a template. Plasmid pAF2 encoding a Ste20p$^{1–298}$ fusion was constructed by amplification of a *Bgl*II–*Xho*I fragment of *STE20* using the oligodeoxy-nucleotides 5′-GATCCTCGACTAAAGATCTTAATGAGCAATGA-TCC-3′ (OKC42; the *Bgl*II site used for cloning is underlined) and OAF1 as primers, and pDH37 as a template. Plasmid pAF3 encoding a Ste20p$^{1–435}$ fusion was created by deletion of the *Sal*I–*Sal*I fragment from plasmid pRL27. Plasmid pRL99 encoding the Ste20p$^{1–435/\Delta 334–369}$ fusion was constructed by replacing the *Bam*HI–*Sal*I fragment of plasmid pAF3 with the *Bam*HI–*Sal*I fragment of plasmid pRS316-STE20(Δ334–369).

Resin binding assays

To create plasmid pAN117, an *Eco*RI–*Bam*HI fragment of *CDC42* was removed from plasmid pRL39 and cloned into plasmid pMAL-p2 (New England Biolabs Inc.) in-frame with the gene encoding maltose binding protein. To create plasmid pGEX-STE20(K649A) encoding a catalytically inactive full-length GST–Ste20p fusion protein, a *Bgl*II–*Xho*I fragment of *STE20*^{K649A} was amplified by PCR using the oligodeoxynucleotides 5′-TCAGATCTATGAGCAATGATCCATCT-3′ and 5′-CCGCTCGAGT-TTACTTTTATCATC-3′ (the newly created *Bgl*II and *Xho*I sites, respect-ively, are underlined) as primers, and pVTU-STE20(K649A) (Wu *et al.*, 1995) as template. The fragment was then cloned into the *Bam*HI and *Xho*I sites of pGEX-4T-3 (Pharmacia Biotech Inc.). To create plasmid pGEX-STE20(Δ334–369), a *Bgl*II–*Xho*I fragment of *STE20*$^{\Delta 334–369}$ was amplified by PCR using the oligodeoxynucleotides 5′-TCAGATCTATG-AGCAATGATCCATCT-3′ and 5′-CCGCTCGAGTTTACTTTTATC-ATC-3′ (the newly created *Bgl*II and *Xho*I sites, respectively, are underlined) as primers, and pVTU-STE20(Δ334–369) as template, and cloned into the *Bam*HI and *Xho*I sites of pGEX-4T-3.

The fusion proteins were expressed in the protease-deficient *E.coli* strain UT5600 (New England Biolabs Inc.). Maltose binding protein–Cdc42p was affinity purified by using amylose–agarose beads in buffer A (20 mM Tris–HCl buffer, pH 7.5, containing 200 mM NaCl, 5 mM EDTA, 1 mM β-mercaptoethanol, 1 mM phenylmethylsulfonyl fluoride, 1 mM pefabloc, 2 μg/ml pepstatin, 2 μg/ml leupeptin, and 2 μg/ml aprotinin), eluted from the beads by incubation in buffer B (50 mM Tris–HCl buffer, pH 7.5, containing 150 mM NaCl, 1.5 mM $MgCl_2$, 1 mM β-mercaptoethanol and 10 mM maltose) for 5 min at room temperature, and stored in aliquots at –70°C. The fusion protein was then loaded with GTPγS or GDPβS by incubating 3 μg of purified protein in 30 μl of buffer C [50 mM Tris–HCl buffer, pH 7.5, containing 4 mM EDTA, 0.5 mM dithiothreitol (DTT), 0.5% bovine serum albumin, 0.1 mM GTPγS or GDPβS] for 15 min at 30°C. The reaction was stopped by adding 10 mM $MgCl_2$ and cooling on ice.

GST–Ste20p fusions were bound to glutathione–Sepharose beads and purified as described (Wu *et al.*, 1995). Five μg of GST–Ste20p bound to the resin were incubated with 3 μg of GTPγS-loaded maltose binding protein–Cdc42p in buffer D (50 mM Tris–HCl buffer, pH 7.5, containing 100 mM NaCl, 5 mM $MgCl_2$, 0.1 mM DTT, 0.2 mM GTP and 0.07% Triton X-100) for 20 min at room temperature. The beads were then washed three times with buffer D, resuspended in Laemmli buffer and separated by SDS–PAGE (Laemmli, 1970). Immunoblots to detect maltose binding protein and Ste20p were then performed as described (Leeuw *et al.*, 1995).

Microscopical analyses

For actin staining, cells were fixed in 3.7% formaldehyde for 20 min at room temperature, washed twice in 10 mM phosphate buffer, pH 7.4, containing 150 mM NaCl (phosphate-buffered saline, PBS), incubated for 45 min at room temperature with 0.5 μM rhodamine–phalloidin in PBS and then washed twice in PBS. For microscopic analyses, a Leica Aristoplan epifluorescence microscope was used with differential interference contrast (Nomarski) optics. Fluorescence of rhodamine and GFP was observed with N2.1 and I3 filters, respectively. Pictures were taken with a Kodak TMAX 400 ASA film.

Assays

Western blot analyses and *in vitro* protein kinase assays were performed as described previously (Wu *et al.*, 1995). β-Galactosidase activities were measured as described, and Miller units were defined as $(OD_{420}\times 1000)/(OD_{600}\times t\times v)$ (Leberer *et al.*, 1992b). Growth inhibition in response to α-factor was determined by 'halo' assays as described previously (Leberer *et al.*, 1994).

Acknowledgements

We wish to thank Doreen Harcus, Robert Larocque and Viktoria Lytvyn for expert technical assistance, and Janet Chenevert, Fatima Cvrckova, Douglas Johnson, Haoping Liu, André Nantel, Roger Y.Tsien and Nicole Valtz for providing yeast strains and plasmids. We also wish to thank Matthias Peter for communicating results prior to publication, and Doreen Harcus and Malcolm Whiteway for critical reading of the manuscript. Work from J.E.S. was supported by a research grant (MCB 9304992) from the US National Science Foundation. The National Research Council of Canada publication number for this work is 39932.

References

Akada,R., Kallal,L., Johnson,D.I. and Kurjan,J. (1996) Genetic relationships between the G protein βγ complex, Ste5p, Ste20p and Cdc42p: investigation of effector roles in the yeast pheromone response pathway. *Genetics*, **143**, 103–117.

Bagrodia,S., Derijard,B., Davis,R.J. and Cerione,R.A. (1995) Cdc42 and PAK-mediated signaling leads to Jun kinase and p38 mitogen-activatd protein kinase activation. *J. Biol. Chem.*, **270**, 27995–27998.

Boeke,J.D., Trueheart,J., Natsoulis,G. and Fink,G.R. (1987) 5-Fluoroorotic acid as a selective agent in yeast molecular genetics. *Methods Enzymol.*, **154**, 164–171.

Brown,J.L., Stowers,L., Baer,M., Trejo,J., Coughlin,S. and Chant,J. (1996) Human Ste20 homologue hPAK1 links GTPases to the JNK MAP kinase pathway. *Curr. Biol.*, **6**, 598–605.

Burbelo,P.D., Drechsel,D. and Hall,A. (1995) A conserved binding motif defines numerous candidate target proteins for both Cdc42 and Rac GTPases. *J. Biol. Chem.*, **270**, 29071–29074.

Chalfie,M., Tu,Y., Euskirchen,G., Ward,W.W. and Prasher,D.C. (1994) Green fluorescent protein as a marker for gene expression. *Science*, **263**, 802–805.

Chang,F. and Herskowitz,I. (1990) Identification of a gene necessary for cell cycle arrest by a negative growth factor of yeast: FAR1 is an inhibitor of a G1 cyclin, CLN2. *Cell*, **63**, 999–1011.

Chant,J. and Stowers,L. (1995) GTPase cascades choreographing cellular behavior: movement, morphogenesis, and more. *Cell*, **81**, 1–4.

Chenevert,J., Corrado,K., Bender,A., Pringle,J. and Herskowitz,I. (1992) A yeast gene (*BEM1*) required for cell polarization whose product contains two SH3 domains. *Nature*, **356**, 77–79.

Chenevert,J., Valtz,N. and Herskowitz,I. (1994) Identification of genes required for normal pheromone-induced cell polarization in *Saccharomyces cerevisiae*. *Genetics*, **136**, 1287–1297.

Chien,C., Bartel,P.L., Sternglanz,R. and Fields,S. (1991) The two-hybrid system: a method to identify and clone genes for proteins that interact with a protein of interest. *Proc. Natl Acad. Sci. USA*, **88**, 9578–9582.

Christianson,T.W., Sikorski,R.S., Dante,M., Shero,J.H. and Hieter,P. (1992) Multifunctional yeast high-copy-number shuttle vectors. *Gene*, **110**, 119–122.

Cvrckova,F., De Virgilio,C., Manser,E., Pringle,J.R. and Nasmyth,K. (1995) Ste20-like protein kinases are required for normal localization of cell growth and for cytokinesis in budding yeast. *Genes Dev.*, **9**, 1817–1830.

Dolan,J.W., Kirkham,C. and Fields,S. (1989) The yeast STE12 protein binds to the DNA sequence mediating pheromone induction. *Proc. Natl Acad. Sci. USA*, **86**, 5703–5707.

Dorer,R., Pryciak,P.M. and Hartwell,L.H. (1995) *Saccharomyces cerevisiae* cells execute a default pathway to select a mate in the absence of pheromone gradients. *J. Cell Biol.*, **131**, 845–861.

Elion,E.A. (1995) Ste5: a meeting place for MAP kinases and their associates. *Trends Cell Biol.*, **5**, 322–327.

Elion,E.A., Trueheart,J. and Fink,G.R. (1995) Fus2 localizes near the site of cell fusion and is required for both cell fusion and nuclear alignment during zygote formation. *J. Cell Biol.*, **130**, 1283–1296.

Frost,J.A., Xu,S., Hutchison,M.R., Marcus,S. and Cobb,M.H. (1996) Actions of Rho family small G proteins and p21-activated protein kinases on mitogen-activated protein kinase family members. *Mol. Cell. Biol.*, **16**, 3707–3713.

Gimeno,C.J., Ljungdahl,P.O., Styles,C.A. and Fink,G.R. (1992) Unipolar cell divisions in the yeast *S.cerevisiae* lead to filamentous growth: regulation by starvation and Ras. *Cell*, **68**, 1077–1090.

Hall,A. (1994) Small GTP-binding proteins and the regulation of the actin cytoskeleton. *Annu. Rev. Cell Biol.*, **10**, 31–54.

Harden,N., Lee,J., Loh,H.-Y., Ong,Y.-M., Tan,I., Leung,T., Manser,E. and Lim,L. (1996) A *Drosophila* homolog of the Rac- and Cdc42-activated serine/threonine kinase PAK is a potential focal adhesion and focal complex protein that colocalizes with dynamic actin structures. *Mol. Cell. Biol.*, **16**, 1896–1908.

Heim,R., Cubitt,A.B. and Tsien,R.Y. (1995) Improved green fluorescence. *Nature*, **373**, 663–664.

Herskowitz,I. (1995) MAP kinase pathways in yeast: for mating and more. *Cell*, **80**, 187–197.

Jackson,C.L., Konopka,J.B. and Hartwell,L.H. (1991) *S.cerevisiae* α pheromone receptors activate a novel signal transduction pathway for mating partner discrimination. *Cell*, **67**, 389–402.

Johnson,D. and Pringle,J.R. (1990) Molecular characterization of *CDC42*, a *Saccharomyces cerevisiae* gene involved in the development of cell polarity. *J. Cell Biol.*, **111**, 143–152.

Jones,J.S. and Prakash,L. (1990) Yeast *Saccharomyces cerevisiae* selectable markers in pUC18 polylinkers. *Yeast*, **6**, 363–366.

Knaus,U.G., Morris,S., Dong,H.-J., Chernoff,J. and Bokoch,G.M. (1995) Regulation of human leukocyte p21-activated kinases through G protein-coupled receptors. *Science*, **269**, 221–223.

Kozma,R., Ahmed,S., Best,A. and Lim,L. (1995) The Ras-related protein Cdc42Hs and bradykinin promote formation of peripheral actin microspikes and filopodia in Swiss 3T3 fibroblasts. *Mol. Cell. Biol.*, **15**, 1942–1952.

Kunkel,T.D., Roberts,J.D. and Zakour,R.A. (1987) Rapid and efficient site-specific mutagenesis without phenotypic selection. *Methods Enzymol.*, **154**, 367–382.

Laemmli,U.K. (1970) Cleavage of structural proteins during the assembly of the head of the bacteriophage T4. *Nature*, **227**, 680–685.

Leberer,E., Dignard,D., Harcus,D., Thomas,D.Y. and Whiteway,M. (1992a) The protein kinase homologue Ste20p is required to link the yeast pheromone response G-protein βγ subunits to downstream signalling components. *EMBO J.*, **11**, 4815–4824.

Leberer,E., Dignard,D., Hougan,L., Thomas,D.Y. and Whiteway,M. (1992b) Dominant-negative mutants of a yeast G-protein β subunit identify two functional regions involved in pheromone signalling. *EMBO J.*, **11**, 4805–4813.

Leberer,E., Dignard,D., Harcus,D., Hougan,L., Whiteway,M. and Thomas,D.Y. (1993) Cloning of *Saccharomyces cerevisiae STE5* as a suppressor of a Ste20 protein kinase mutant: structural and functional similarity of Ste5 to Far1. *Mol. Gen. Genet.*, **241**, 241–254.

Leberer,E., Dignard,D., Harcus,D., Whiteway,M. and Thomas,D.Y. (1994) Molecular characterization of *SIG1*, a *Saccharomyces cerevisiae* gene involved in negative regulation of G-protein-mediated signal transduction. *EMBO J.*, **13**, 3050–3064.

Leberer,E., Chenevert,J., Leeuw,T., Harcus,D., Herskowitz,I. and Thomas,D.Y. (1996) Genetic interactions indicate a role for Mdg1p and SH3 domain protein Bem1p in linking the G-protein mediated yeast pheromone signalling pathway to regulators of cell polarity. *Mol. Gen. Genet.*, **252**, 608–621.

Leeuw,T., Fourest,A., Wu,C., Chenevert,J., Clark,K., Whiteway,M., Thomas,D.Y. and Leberer,E. (1995) Pheromone response in yeast: association of Bem1p with proteins of the MAP kinase cascade and actin. *Science*, **270**, 1210–1213.

Lipke,P.N. and Kurjan,J. (1992) Sexual agglutinins in budding yeasts: structure, function and regulation of yeast cell adhesion proteins. *Microbiol. Rev.*, **56**, 180–194.

Liu,H., Styles,C. and Fink,G.R. (1993) Elements of the yeast pheromone response pathway required for filamentous growth of diploids. *Science*, **262**, 1741–1744.

Manser,E., Leung,T., Salihuddin,H., Tan,L. and Lim,L. (1993) A non-receptor tyrosine kinase that inhibits the GTPase activity of $p21^{cdc42}$. *Nature*, **363**, 364–367.

Manser,E., Leung,T., Salihuddin,H., Zhao,Z. and Lim,L. (1994) A brain serine/threonine protein kinase activated by Cdc42 and Rac1. *Nature*, **367**, 40–46.

Martin,G.A., Bollag,G., McCormick,F. and Abo,A. (1995) A novel serine kinase activated by rac1/CDC42Hs-dependent autophosphorylation is related to PAK65 and STE20. *EMBO J.*, **14**, 1970–1978.

McCaffrey,G., Clay,F.J., Kelsay,K. and Sprague G.F.,Jr (1987) Identification and regulation of a gene required for cell fusion during mating of the yeast *Saccharomyces cerevisiae*. *Mol. Cell. Biol.*, **7**, 2680–2690.

Mösch,H.-U., Roberts,R.L. and Fink,G.R. (1996) Ras2 signals via the Cdc42/Ste20/mitogen-activated protein kinase module to induce filamentous growth in *Saccharomyces cerevisiae*. *Proc. Natl Acad. Sci. USA*, **93**, 5352–5356.

Nobes,C.D. and Hall,A. (1995) Rho, Rac, and Cdc42 GTPases regulate the assembly of multimolecular focal complexes associated with actin stress fibers, lamellipodia, and filopodia. *Cell*, **81**, 53–62.

Peterson,J., Zheng,Y., Bender,L., Myers,A., Cerione,R. and Bender,A. (1994) Interactions between the bud emergence proteins Bem1p and Bem2p and Rho-type GTPases in yeast. *J. Cell Biol.*, **127**, 1395–1406.

Polverino,A., Frost,J., Yang,P., Hutchison,M., Neiman,A.M., Cobb,M.H. and Marcus,S. (1995) Activation of mitogen-activated protein kinase cascades by p21-activated protein kinases in cell-free extracts of *Xenopus* oocytes. *J. Biol. Chem.*, **270**, 26067–26070.

Pombo,C.M., Kehrl,J.H., Sanchez,I., Katz,P., Avruch,J., Zon,L.I., Woodgett,J.R., Force,T. and Kyriakis,J.M. (1995) Activation of the SAPK pathway by the human *STE20* homologue germinal centre kinase. *Nature*, **377**, 750–754.

Ramer,S.W. and Davis,R.W. (1993) A dominant truncation allele identifies a gene, *STE20*, that encodes a putative protein kinase necessary for mating in *Saccharomyces cerevisiae*. *Proc. Natl Acad. Sci. USA*, **90**, 452–456.

Ramezani Rad,M., Xu,G. and Hollenberg,C.P. (1992) *STE50*, a novel gene required for activation of conjugation at an early step in mating in *Saccharomyces cerevisiae*. *Mol. Gen. Genet.*, **236**, 145–154.

Roberts,R.L. and Fink,G.R. (1994) Elements of a single MAP kinase cascade in *Saccharomyces cerevisiae* mediate two developmental programs in the same cell type: mating and invasive growth. *Genes Dev.*, **8**, 2974–2985.

Rose,M.D., Winston,F. and Hieter,P. (1990) *Methods in Yeast Genetics: A Laboratory Manual*. Cold Spring Harbor Laboratory Press, Cold Spring Harbor, NY.

Saiki,R.J., Gelfand,D.H., Stoffel,S., Scharf,S.J., Higuchi,R., Horn,G.T., Mullis,K.B. and Erlich,H.A. (1988) Primer-directed enzymatic amplification of DNA with a thermostable DNA polymerase. *Science*, **239**, 487–491.

Segall,J.E. (1993) Polarization of yeast cells in spatial gradients of α-mating factor. *Proc. Natl Acad. Sci. USA*, **90**, 8332–8336.

Sikorski,R.S. and Hieter,P. (1989) A system of shuttle vectors and yeast host strains designed for efficient manipulation of DNA in *Saccharomyces cerevisiae*. *Genetics*, **122**, 19–27.

Simon,M.-N., De Virgilio,C., Souza,B., Pringle,J.R., Abo,A. and Reed,S.I. (1995) Role for the Rho-family GTPase Cdc42 in yeast mating-pheromone signal pathway. *Nature*, **376**, 702–705.

Stevenson,B.J., Ferguson,B., De Virgilio,C., Bi,E., Pringle,J.R., Ammerer,G. and Sprague,G.F.,Jr (1995) Mutation of RGA1, which encodes a putative GTPase-activating protein for the polarity-establishment protein Cdc42p, activates the pheromone-response pathway in the yeast *Saccharomyces cerevisiae*. *Genes Dev.*, **9**, 2949–2963.

Symons,M., Derry,J.M.J., Karlak,B., Jiang,S., Lemahieu,V., McCormick,F., Francke,U. and Abo,A. (1996) Wiskott–Aldrich syndrome protein, a novel effector for the GTPase CDC42Hs, is implicated in actin polymerization. *Cell*, **84**, 723–734.

Teo,M., Manser,E. and Lim,L. (1995) Identification and molecular cloning of a $p21^{cdc42/rac1}$-activated serine/threonine kinase that is rapidly activated by thrombin in platelets. *J. Biol. Chem.*, **270**, 26690–26697.

Trueheart,J.D., Boeke,J.D. and Fink,G.R. (1987) Two genes required for cell fusion during yeast conjugation: evidence for a pheromone-induced surface protein. *Mol. Cell. Biol.*, **7**, 2316–2328.

Valtz,N., Peter,M. and Herskowitz,I. (1995) FAR1 is required for oriented polarization of yeast cells in response to mating pheromones. *J. Cell Biol.*, **131**, 863–873.

Whiteway,M.S., Wu,C., Leeuw,T., Clark,K., Fourest,A., Thomas,D.Y. and Leberer,E. (1995) Association of the yeast pheromone response G protein βγ subunits with the MAP kinase scaffold Ste5p. *Science*, **269**, 1572–1575.

Wu,C., Whiteway,M., Thomas,D.Y. and Leberer,E. (1995) Molecular characterization of Ste20p, a potential mitogen-activated protein or extracellular signal-regulated kinase kinase (MEK) kinase kinase from *Saccharomyces cerevisiae*. *J. Biol. Chem.*, **270**, 15984–15992.

Zarzov,P., Mazzoni,C. and Mann,C. (1996) The SLT2(MPK1) MAP kinase is activated during periods of polarized cell growth in yeast. *EMBO J.*, **15**, 83–91.

Zhao,Z.-S., Leung,T., Manser,E. and Lim,L. (1995) Pheromone signalling in *Saccharomyces cerevisiae* requires the small GTP-binding protein Cdc42p and its activator *CDC24*. *Mol. Cell. Biol.*, **15**, 5246–5257.

Zheng,Y., Cerione,R. and Bender,A. (1994) Control of the yeast bud-site assembly GTPase Cdc42: catalysis of guanine-nucleotide exchange by Cdc24 and stimulation of GTPase activity by Bem3. *J. Biol. Chem.*, **28**, 2369–2372.

Ziman,F.J.M., O'Brien,M., Ouellette,L.A., Church,W.R. and Johnson,D.I. (1991) Mutational analysis of *CDC42Sc*, a *Saccharomyces cerevisiae* gene that encodes a putative GTP-binding protein involved in the control of cell polarity. *Mol. Cell. Biol.*, **11**, 3537–3544.

Ziman,M., Preuss,D., Mulholland,J., O'Brien,J.M., Botstein,D. and Johnson,D.I. (1993) Subcellular localization of Cdc42p, a *Saccharomyces cerevisiae* GTP-binding protein involved in the control of cell polarity. *Mol. Biol. Cell*, **4**, 1307–1316.

Received on July 31, 1996; revised on September 13, 1996